Pressure driven magnetic order in Sr <inf>1</inf><inf>-</inf><inf>x</inf> Ca <inf>x</inf> Co <inf>2</inf> P <inf>2</inf>

scientific reports

Check for updates

OPEN

Pressure driven magnetic order in $Sr_{1-x}Ca_xCo_2P_2$

Ola Kenji Forslund[1]✉, Daniel Andreica[2], Yasmine Sassa[3], Masaki Imai[4], Chishiro Michioka[4], Kazuyoshi Yoshimura[4], Zurab Guguchia[5], Zurab Shermadini[5], Rustem Khasanov[5], Jun Sugiyama[6] & Martin Månsson[1]

The magnetic phase diagram of $Sr_{1-x}Ca_xCo_2P_2$ as a function of hydrostatic pressure and temperature is investigated by means of high pressure muon spin rotation, relaxation and resonance (μ^+SR). The weak pressure dependence for the $x \neq 1$ compounds suggests that the rich phase diagram of $Sr_{1-x}Ca_xCo_2P_2$ as a function of x at ambient pressure may not solely be attributed to chemical pressure effects. The $x = 1$ compound on the other hand reveals a high pressure dependence, where the long range magnetic order is fully suppressed at $p_{c2} \approx 9.8$ kbar, which seem to be a first order transition. In addition, an intermediate phase consisting of magnetic domains is formed above $p_{c1} \approx 8$ kbar where they co-exist with a magnetically disordered state. These domains are likely to be ferromagnetic islands (FMI) and consist of an high- (FMI-①) and low-temperature (FMI-②) region, respectively, separated by a phase boundary at $T_i \approx 20$ K. This kind of co-existence is unusual and is originating from a coupling between lattice and magnetic degrees of freedoms.

The $ThCr_2Si_2$ layered structure type family of compounds typically exhibits ground states ranging from superconductivity to long range magnetic order[1–5]. The ground states are determined by competition between magnetism and superconductivity, as in $CaFe_2As_2$ or $Ba_{1-x}K_xFe_2As_2$[6,7]. In this family, the AM_2X_2 structure type with a metal A, transition metal M, and metalloid X atoms, are made up of edge-share TMX_4 tetrahedra layers (inset of Fig. 7a). The delicate ground state is mostly dependent on the inter-layer X-X bonding distance across the intermediate A sheets. For several AM_2P_2 (A = Ca, Sr, and Ba, and M = Fe, Co, and Ni) materials, the phase transitions are related to subtle structural changes present in the crystals. In particular, these families have a tendency to transform from uncollapsed tetragonal (ucT) to collapsed tearagonal (cT) structure. This is driven by the X-X bonding acting between the M_2X_2 layers, for which strong enough bonds pull the layers closer and induces a lattice relaxation[8–10].

In the case of $Sr_{1-x}Ca_xCo_2P_2$, the crystals transforms from ucT to cT when the chemical composition changes from $x = 0$ to $x = 1$. A Curie-Weiss behaviour is observed in all compounds at high temperature, but the high temperature fluctuations changes from antiferromagnetic to ferromagentic type around $x \sim 0.5$[10]. Such change seem to be correlated to the finally ground state as it is transformed from paramagnetic ($x < 0.45$) to antiferromagnteic (AF) at $x \approx 0.5$[11]. In fact, bulk magnetisation measured as a function of x show a clear correlation between the detailed crystalline structure and the magnetic properties[10].

Previous study based on muon spin rotation, relaxation and resonance (μ^+SR)[11] have indicated Pauli-paramagnetic phases for $x < 0.45$ at temperatures as low as 1.8 K. Short-range AF ordered phases appears for $0.48 \leq x \leq 0.75$, which stabilizes into a long-range AF ordered phase for $x > 0.75$. The formation of magnetically ordered phases was shown to have strong correlations with the nearest neighboring Co distance (d_{Co-Co}) within the Co_2P_2 planes, implying the importance of also the inter-plane interaction for the formation of long range order. The Co–Co distance decreases only moderately with x up until ~ 0.5, at which point d_{Co-Co} experience an abrupt decrease until $x \sim 0.9$ where it finally levels out to an almost constant value[11].

It is thus interesting to continue the investigation by further decreasing the distance d_{Co-Co} through the application of a hydrostatic pressure. Such study was performed on $CaCo_2P_2$ single crystals using resistivity[12]. These measurements suggested that the AF order is suppressed with pressure, hinting towards the existence of a quantum critical point (QCP). Moreover, the signature of a second unknown phase was also indicated in the pressurised state, but the details of such phase remain unknown.

[1]Department of Applied Physics, KTH Royal Institute of Technology, 106 91 Stockholm, Sweden. [2]Faculty of Physics, Babes-Bolyai University, 400084 Cluj-Napoca, Romania. [3]Department of Physics, Chalmers University of Technology, 41296 Göteborg, Sweden. [4]Department of Chemistry, Graduate School of Science, Kyoto University, Kyoto 606-8502, Japan. [5]Laboratory for Muon Spin Spectroscopy, Paul Scherrer Institute (PSI), 5232 Villigen, Switzerland. [6]Neutron Science and Technology Center, Comprehensive Research Organization for Science and Society (CROSS), Tokai, Ibaraki 319-1106, Japan. ✉email: olake@chalmers.se

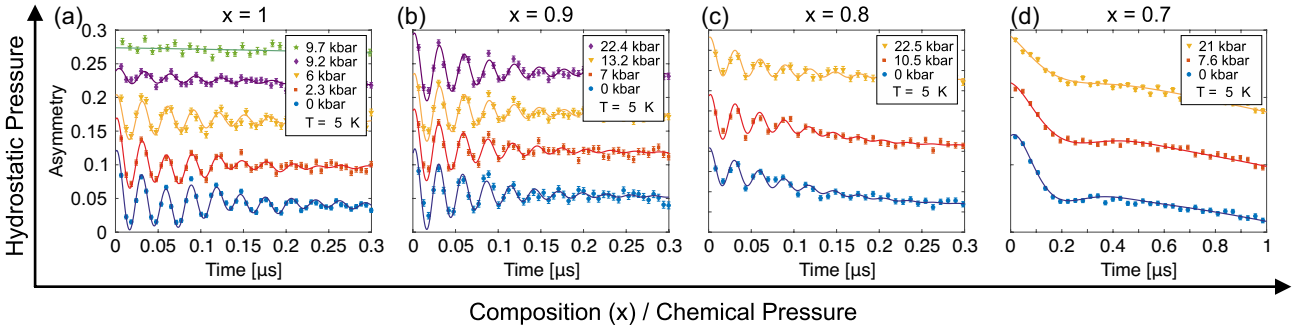

Figure 1. Zero field time spectra collected at selected pressures at $T = 5$ K for the $Sr_{1-x}Ca_xCo_2P_2$ compounds: (**a**) $x = 1$, (**b**) $x = 0.9$, (**c**) $x = 0.8$ and (**d**) $x = 0.7$. The solid lines represents fits using Eq. (1). Each spectra have been shifted vertically for clarity of display.

In order to confirm and further comprehend the high pressured states, we have conducted pressure dependent μ^+SR measurements on the series of $Sr_{1-x}Ca_xCo_2P_2$ powder samples, including $x = 1$, 0.9, 0.8 and 0.7. The overall results are summarised in form of a composition-pressure-temperature phase diagram in Fig. 7. A strong pressure dependence is observed for the $x = 1$ compound for which the magnetic order is completely suppressed around $p_{c2} \approx 9.8$ kbar. This suppression is associated with co-existence of magnetic order and disorder just below p_{c2}, for which the origin is discussed below. Given that μ^+SR is highly sensitive to magnetic fields and to magnetic volume fractions, any subtle magnetic transition can be detected and characterized in detail.

Results

Series of μ^+SR measurements on $Sr_{1-x}Ca_xCo_2P_2$ are presented as a function of pressure, temperature and chemical composition ($x = 1$, 0.9, 0.8 and 0.7). In particular, measurements in weak transverse field (TF) configuration are used in other to estimate the phase boundaries, while zero field (ZF) measurements are employed to deduce the detailed magnetic ground state. Transverse refers to the direction of the externally applied field, which is perpendicular with respect to the initial muon spin polarisation.

Zero field. Figure 1 displays the collected ZF μ^+SR time spectra at $T = 5$ K for the compositions $x = 1$, 0.9, 0.8 and 0.7 as a function of pressure. A strong pressure dependence is observed for the $x = 1$ compound. Indeed, several oscillations are present in the time spectra for $p \leq 9.2$ kbar, where the number of frequencies as well as the amplitude of the oscillations decreases with the applied pressure. Such oscillations are fully suppressed for $p_{c2} \geq 9.7$ kbar. A much more moderate pressure dependence is observed for the other compositions ($x = 0.9$, 0.8 and 0.7). Consequently, it is initially clear that the ZF time spectra has a strong x dependence, while the most evident hydrostatic pressure effect seem to be limited to $x = 1$ compound. In order to more systematically characterize the detailed changes across x and p, the time spectra were fitted using a combination of several exponentially relaxing oscillations, an exponential and a static Gaussian Kubo-Toyabe (SGKT):

$$\begin{aligned} A_0\, P_{\mathrm{ZF}}(t) = &\sum_i^n A_i^{\mathrm{AF}} \cos(f_i^{\mathrm{AF}} 2\pi t + \phi_i^{\mathrm{AF}}) e^{-\lambda_i^{\mathrm{AF}} t} \\ &+ A_{\mathrm{tail}} e^{-\lambda_{\mathrm{tail}} t} + A_{\mathrm{PC}} G(t, \Delta_{\mathrm{PC}}) e^{-\lambda_{\mathrm{PC}} t} \\ &+ A_{\mathrm{PM}} e^{-\lambda_{\mathrm{PM}} t}, \end{aligned} \tag{1}$$

where A_0 is the initial asymmetry, determined by the instrument, and P_{ZF} is the muon spin polarisation function in ZF configuration. In detail, the number of oscillations, $n = 3$ and $n = 2$, where used for the compositions $x = 1$ and $x = 0.8$, respectively, while $n = 1$ was used for both $x = 0.9$ and $x = 0.7$. The number of oscillations, *i.e.* n, depends on the number of magnetically different muon site in the compound. It depends on the detailed coupling between the internal magnetic field, generated by the magnetic structure, and on the available crystallographic muon site, which depends on the crystal structure. A_i^{AF}, f_i^{AF}, ϕ_i^{AF} and λ_i^{AF} are the asymmetry, precession frequency, phase and relaxation rate for the internal field component that is perpendicular with respect to the initial muon spin polarisation. A_{tail} and λ_{tail} on the other hand are the asymmetry and relaxation rate of the so called tail component, *i.e.* the internal field component that is parallel to the initial muon spin polarisation. In a perfect powder that is magnetically ordered, 2/3 of the internal field components are expected to be perpendicular while 1/3 of the internal field components are parallel to the initial muon spin polarization (due to the so-called 'powder average'). A_{PM}, and λ_{PM} are accounting for the new high pressure paramagnetic (PM) phase of the $x = 1$ compound that is not magnetically ordered (Fig. 1a). A_{PC}, Δ_{PC} and λ_{PC} on the other hand are the asymmetry, the field distribution width and the corresponding exponential relaxation rate of the static Gaussian KT, represented by $G(t, \Delta)$, of the pressure cell (PC). Here, $G(t, \Delta)$ originates from isotropically distributed magnetic moments while the exponential accounts for additional relaxation present on top of it[13]. Such description holds for when the internal field is composed of two separate and independent magnetic field origins. In such case, the Fourier transform of the convolution of each field distribution is the product of each polarisation functions. In other

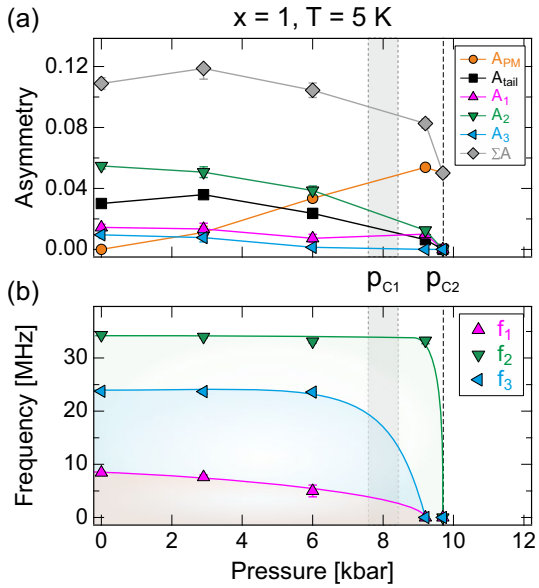

Figure 2. Pressure dependent fit parameters, collected at $T = 5$ K, of the $x = 1$ compound obtained through Eq. (1). For reference, $\sum A = \sum A_i^{\mathrm{AF}} + A_{\mathrm{tail}} + A_{\mathrm{PM}}$ has been computed and is included as well. The solid lines are guide to the eye while the vertical shaded area and dashed line indicate the critical pressures, $p_{c1} \approx 8$ kbar and $p'_{c2} \approx 9.5$ kbar.

words, the KT accounts for the field distribution created by isotropically distributed nuclear moments while the exponential accounts for additional relaxation posed by highly fluctuating electronic moments.

The constraint $A_{\mathrm{tail}} = \frac{1}{2}\sum A_i^{\mathrm{AF}}$ (*i.e.* 1/3 vs. 2/3) was set for the fitting procedures using Eq. (1), in order to separate the various contributions present for $p > 0$. Moreover, the compounds are known to exhibit a commensurate magnetic order. Indeed, $\phi_1 = -20.0(2.9)^\circ$, $\phi_2 = -10.6(10.4)^\circ$ and $\phi_3 = -28.7(16.6)^\circ$ are obtained for the compound $x = 1$ at $p = 0$, consistent with a commensurate order. Therefore, a common phase was set, *i.e.* $\phi_i = \phi$, across all oscillations for all measured pressures. Using the described fitting procedure, the pressure dependencies of the obtained fit parameters for the $x = 1$ compound are shown in Fig. 2.

At ambient pressure $A_{\mathrm{tail}} \simeq \frac{1}{2}\sum A_i^{\mathrm{AF}}$ is obtained, suggesting that the constraint set for higher pressures is valid. For higher pressures, the asymmetries A_i^{AF} decrease gradually as the A_{PM} component increases. It should be noted that the total sample asymmetry ($\sum A = \sum A_i^{\mathrm{AF}} + A_{\mathrm{tail}} + A_{\mathrm{PM}}$) shows a fairly constant behaviour up to about 6 kbar. At higher pressures, a sudden decrease is observed. The origin of this behaviour is highlighted in Fig. 3. As clearly seen, a significant missing fraction presents itself at higher pressures. Since a missing fraction cannot be fitted (since it lies outside the accessible time frame of the μ^+SR instrument), the total sample asymmetry ($\sum A$) exhibits a decrease as a function of pressure. The origin of this missing fraction is discussed below. A_{PM} on the other hand represents the volumic fraction of non-magnetically ordered state, *e.g.* paramagnetic or spin liquid. Such high pressure state is discussed in "Discussion".

Pressure has a weak effect on the order parameter of the system (Fig. 2b), which is the precession frequency and corresponds to the local magnetic field at the muon site. The main frequency, f_2, maintains more or less the value at ambient pressure (~ 34 MHz) up to 9.2 kbar (~ 33 MHz). We may initially define the pressure point at which all precession frequencies are absent as the critical pressure, $p'_{c2} \approx 9.5$ kbar. We will further refine such critical point based on the TF measurement presented below. It is noted that the 24 MHz (f_3) frequency was not present in the previous ambient pressure study[11]. Most likely, the $x = 1$ sample of the present study is both much larger and of higher quality, resulting in that even the minor frequency can be distinguished. That being said, the inclusion of such frequency does not change/alter the interpretation of this or the previous study.

Two of the precession frequencies, f_1 and f_3, drop to 0 MHz already at $p_{c1} \approx 8$ kbar, *i.e.* prior to the vanishing of the f_2 component at $p'_{c2} \approx 9.5$ kbar. It is however clear that the asymmetry (A_1^{AF}) still poses non-zero values. In other words, the depolarisation of this component is a fast exponential instead of an oscillation. This behaviour suggests a widening of the internal field distribution width in which the oscillation becomes highly damped. This would be consistent with a spin reorientation, structural transition (*i.e.* muon sites changes) and/or it could reflect a difficulty in fitting small asymmetries. However, we will later show (below) that this effect is indeed a true sample effect and not related to a fitting problem.

While it is not shown, the relaxation rates, λ_i^{AF}, show a weak pressure dependence. Roughly put, a value of $\lambda_i^{\mathrm{AF}} \simeq 9\ \mu\mathrm{s}^{-1}$ is obtained for all oscillation across all pressures. λ_{tail} on the other hand exhibits low or values close to 0 across all pressures, suggesting a static magnetic ground state. λ_{PM} on the other hand increases for $p > 2.3$ kbar, suggesting that the high pressure phase is dynamic in origin.

A significant fraction is missing for the $x = 1$ compound at higher pressures, *i.e.* the total asymmetry does not add up to values close to A_0. This is directly highlighted in Fig. 3, which shows the ZF time spectra collected at 5 and 35 K for 9.7 kbar and at $T = 0.3$ K for $p = 17.2$ kbar. The 5 K time spectrum is identical to the one shown

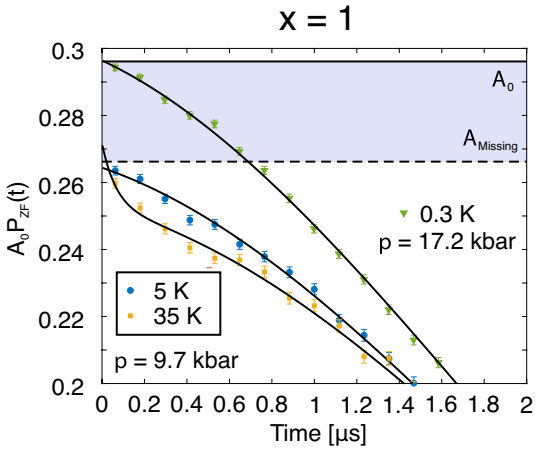

Figure 3. Zero field time spectra collected at $T = 5$ and 35 K at $p = 9.7$ kbar (yellow and blue) and $T = 0.3$ K at $p = 17.2$ kbar (green) for the $x = 1$ compound. The solid lines represents fits using Eq. (1) with $n = 1$ but with $f_1 = 0$ MHz for $T = 35$ K and $n = 0$ for $T = 5$ K. The horizontal solid black line is the estimated A_0 while the missing fraction ($A_missing$) is the band between A_0 the dashed black horizontal line. The $p = 17.2$ kbar spectra was collected using a different cryostat and the spectra were shifted down by 0.13 units to match the estimated A_0 for the nominal cryostat of this study (the specific value of A_0 is cryostat dependent).

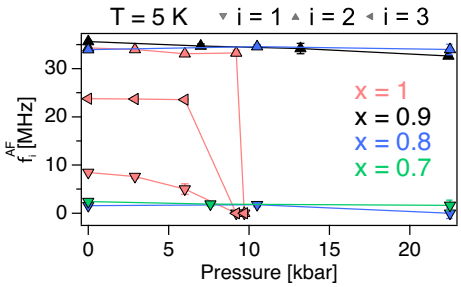

Figure 4. Pressure dependent precession frequencies, collected at $T = 5$ K, of $Sr_{1-x}Ca_xCo_2P_2$ compounds obtained through Eq. (1): $x = 1$ (light pink), 0.9 (black), 0.8 (blue) and 0.7 (green). The solid lines are guide to the eye.

in Fig. 1a. While the 5 K time spectrum show no significant signature, the 35 K time spectrum manifests a fast relaxing exponential. Perhaps a dip/minimum is present in Fig. 3 around 0.5 μs, suggesting that the polarisation function is more of an oscillation rather than an exponential. However, a fit with a cosine function yields unreasonably high asymmetry values. Regardless, the fraction of this fast exponential decreases with decreasing temperature. Such behaviour is the origin behind the complex temperature dependence of A_{TF} at lower temperatures (Fig. 6a). In fact, resistivity measurements under pressure indicated a sudden change in the derivative of the resistivity around this temperature and pressure[12] and is discussed in "Discussion".

Typically, missing fractions are associated with muonium formations[14–16] or by a presence of quasi-static wide field distribution. Since the $x = 1$ compound is metallic even under pressure, muonium formation is unlikely. Instead, the missing fraction originates from a wide internal field distribution yielding oscillations and fluctuations outside the time resolution of μ^+SR. Such a scenario is consistent with having muon sites close to CoP_2 tetrahedra layers giving wide field distributions due to slowly fluctuating Co d-moments. Similar missing fraction effect was observed *e.g.* in the 2D AF magnet $NaNiO_2$[17], which was shown to originate from quasi static wide field distributions at the muon site close to the Ni-O octahedra. In other words, the suppression of the oscillating asymmetries (Fig. 2a) is consistent with changes in the magnetic characteristics at high pressure such that the magnetic field distributions at the muon site increases. Given the crystal flexibility of the $x = 1$ compound, it could also be that additional energetically favorable crystalline muon sites becomes available under higher pressure instead (i.e. the crystalline muon site changes). Such assertion is ideally confirmed by a combination of high pressure XRD and DFT calculations. Regardless of the driver for the missing fraction, it is clear that its origin is related to intrinsic magnetism of the sample since the missing fraction is in fact absent in the $p = 17.2$ kbar measurement (Figs. 3 and 6).

For the sake of completeness, the pressure dependent precession frequencies for all measured x is presented in Fig. 4. The frequencies of the $x = 1$ compound are the same as presented in Fig. 2b. The main frequency of about 34 MHz is present for $x \geq 0.8$. Such frequency is a consequence of the long range order present at ambient

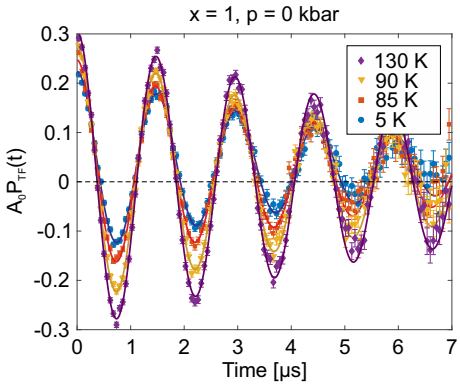

Figure 5. Transverse field (TF = 50 Oe) μ^+SR time spectra collected for $CaCo_2P_2$ ($x = 1$) at $p = 0$ kbar for selected temperatures. The solid lines represents fits with Eq. (2).

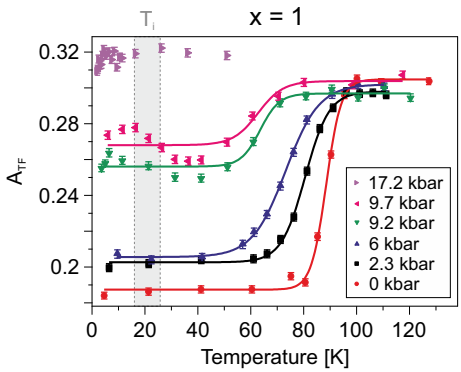

Figure 6. Temperature and pressure dependence of A_{TF} for the $x = 1$ compound, obtained using Eq. (2). The solid lines are fits using the sigmoidal function, while the vertical shaded area indicate an approximative region for the transition temperature $T_i \approx 20$ K (see text and Fig. 7 for further details).

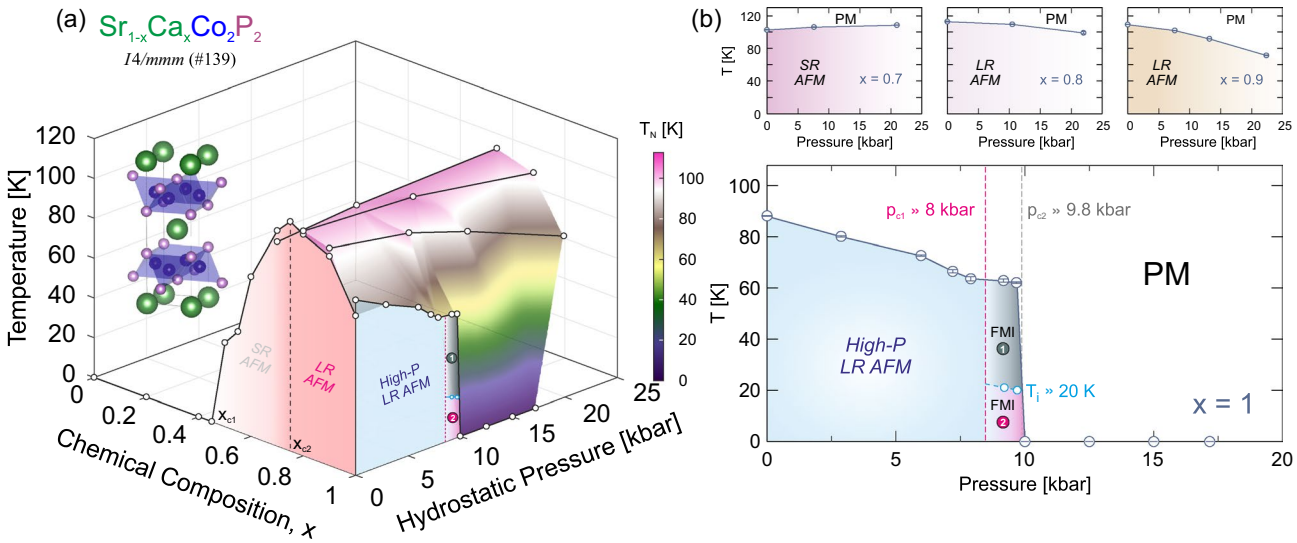

Figure 7. (**a**) Phase-diagram ($p/T/x$) for $Sr_{1-x}Ca_xCo_2P_2$. (**b**) Individual p/T phase diagrams for different chemical compositions (x). Phases are labelled: *SR* short-range, *LR* long-range, *AFM* antiferromagnetic, *FMI* ferromagnetic islands, *PM* paramagnetic. Further, $p_{c1} \approx 8$ kbar and $p_{c2} \approx 9.8$ kbar are the critical pressures and $x_{c1} \approx 0.45$ and $x_{c2} \approx 0.75$ critical chemical compositions[11]. Finally, $T_i \approx 20$ K is an approximate transition temperature between the FMI-① and FMI-② phases.

pressure for $x \geq 0.8$[11]. At $x = 0.8$ however, an additional frequency appears around 2 MHz. Such frequency is concluded to be associated with a short-range order based on the fact that the same frequency but as a highly damped oscillation is present for the $x = 0.7$ sample[11]. Perhaps $x = 0.8$ exhibits a co-existence of short and long range order, similar to in the isostructural compound $LaCo_2P_2$[18]. Regardless though, only weak shifts in the precession frequencies are observed as a function of pressure for $x < 1$. Similarly, the asymmetries and depolarisation rates show only weak pressure dependence, as already hinted directly from Fig. 1b–d.

Transverse field. In order to gain a more detailed insights of the temperature dependent behaviour, the series of compounds were also studied under TF configuration for selected pressures. Figure 5 shows the collected TF ($\sim$ 50 Oe) μ^+SR time spectra from the $x = 1$ compound at $p = 0$ for selected temperatures. Regardless of temperature, a single distinct oscillation of about 0.7 MHz is observed, corresponding to the externally applied field of 50 Oe. A strong temperature dependence in the amplitude is seen, reflecting the formation of static internal magnetic fields. Moreover, the time spectra exhibits a positive shift in asymmetry at lower temperatures. Therefore, the TF time spectra were fitted using a combination of one exponentially relaxing oscillation together with a non oscillating exponential:

$$\begin{aligned} A_0\, P_{\mathrm{TF}}(t) =& A_{\mathrm{TF}} \cos(f_{\mathrm{TF}} 2\pi t + \phi_{\mathrm{TF}}) e^{-\lambda_{\mathrm{TF}} t} \\ &+ A_{\mathrm{S}} e^{-\lambda_{\mathrm{S}} t}, \end{aligned} \tag{2}$$

where A_0 is the initial asymmetry determined by the instrument and P_{TF} is the muon spin polarisation function in TF configuration. A_{TF}, f_{TF}, ϕ_{TF} and λ_{TF} are the asymmetry, frequency, phase and depolarisation rate resulting from the applied TF, while A_{S} and λ_{S} are the asymmetry and the relaxation rate resulting from internal magnetic field components, that is mostly parallel to the initial muon spin. The perpendicular internal magnetic field components are excluded from Eq. (2), since such contribution are usually difficult to model in TF configuration due to the low statistics and the binning of the data. Excluding such contribution does not affect the fit results nor the interpretation of the data.

The temperature dependencies of the obtained TF asymmetry using Eq. (2) are displayed in Fig. 6 for the $x = 1$ compound. A_{TF} has a temperature dependence expected for a magnetically ordered sample. At low temperatures A_{TF} experiences a temperature independent behaviour. As the temperature increases, an increase in A_{TF} is observed and full asymmetry (A_0) is recovered. Ideally, the normalized A_{TF}/A_0 should correspond to the paramagnetic volume fraction of the system. In this case, it is in fact the non-magnetically ordered volume fraction of the sample together with the fraction of muons stopping inside the pressure cell. In other words, the increase of A_{TF} corresponds to the transition temperature ($T_{\mathrm{N}}^{\mathrm{TF}}$) in which the sample changes from a magnetically ordered to disordered state. An accurate value of $T_{\mathrm{N}}^{\mathrm{TF}}$ is obtained by employing sigmoidal fit function as a function of temperature for each measured pressure. The pressure dependent values [i.e. $(T_{\mathrm{N}}^{\mathrm{TF}}(p, x)$] are then utilized to contruct the detailed phase diagram presented in Fig. 7. Intriguingly, A_{TF} show a complex temperature dependence below $T_{\mathrm{N}}^{\mathrm{TF}}$ for the measurements performed at $p = 9.2$ and 9.7 kbar. In fact some of the TF asymmetry (A_{TF}) seems to be recovered around $T_{\mathrm{i}} \approx 20$ K (Fig. 6). Such complexity is reflecting the fact that an initial faster relaxation is present at higher temperature in ZF (Fig. 3). That A_{TF} still exhibits a drop at T_{N} is evidence of static internal field formation, which in ZF configuration resulted into a missing fraction as described above. As mentioned, this fraction stems from muons experiencing very broad field distribution width. At the highest pressure on the other hand, no significant temperature dependence is observed, suggesting the absence of magnetic order at lower temperatures. A similar complicated $A_{\mathrm{TF}}(T)$ behaviour is not observed in any of the other ($x \neq 1$) compounds.

Phase diagram. Based on the presented pressure dependent results, and from previous ambient pressure study[11], a $T/p/x$ phase diagram for $Sr_{1-x}Ca_xCo_2P_2$ can be constructed (Fig. 7a). In general, the detailed ground state is estimated from the ZF measurements while the temperature boundary is estimated from TF configuration. The transition temperatures, based on TF measurements, are presented in Fig. 7 as a function of pressure. As already pointed out, a strong pressure dependence is observed for the $x = 1$ compound. The transition temperature decreases linearly with pressure, until it is completely and suddenly suppressed around $p_{c2} \approx 9.8$ kbar. Such critical pressure is fully coherent with the ZF frequency dependence presented above in Fig. 2b. Further, both ZF (Fig. 2) and TF (Fig. 6) data show signatures for additional phases (FMI-① and FMI-②) appearing already at pressures in the vicinity of $p_{c1} \approx 8$ kbar and $T_{\mathrm{i}} \approx 20$ K. The origin of such phases are further discussed below in "Discussion".

A linear like decrease in the transition temperature is also observed for the $x = 0.9$ and $x = 0.8$ compounds (Fig. 7b). While the magnetic order is persistent within the current pressure range, most likely, the long range order will be destroyed at higher pressures. The pressure dependence of the $x = 0.7$ compound, which is on the left side of the $T_{\mathrm{N}}(x)$ dome (Fig. 7), is opposite from the other ones. Instead of a decrease in transition temperature, the pressure slightly increases T_{N}, suggesting that the magnetic order is stabilized under pressure. Such behaviour is consistent with the results obtained at ambient pressure, where the T_{N} of $x = 0.7$ is lower than that of $x = 0.75$, at which point a long range magnetic order is stabilised[11]. In other words, chemical pressure (and hydrostatic pressure) stabilises the magnetic order for $x < 0.75$ until a long range order is stabilised. That being said, the ZF time spectra (Fig. 1d) and the fit results show no apparent change with pressure. Therefore, a short range order can be expected up to at least 20 kbar for the $x = 0.7$ compound.

Discussion

Given that no significant pressure dependence is observed for $x \neq 1$ compounds, we may attribute the high pressure ground state (up to 20 kbar) to be the same as in ambient pressure. Previous ambient pressure μ^+SR study[11] as a function of x determined the formation of short range AF order for $0.45 < x \leq 0.75$, which develops into an long range AF order for higher x. Such finding is consistent with this study, where distinct oscillations are present for $x > 0.7$ compounds, but only a single highly damped oscillation is present for the $x = 0.7$ compound. The magnetic order formation was found to be strongly correlated with the distance from the Co ions and the adjacent Co_2P_2 planes (d_{Co-Co}); a linear decrease in d_{Co-Co} is observed from about $x = 0.4$ up to about $x = 0.8$[11].

If the magnetic order is truly only dependent on d_{Co-Co}, then one would expect the formation of long range order at higher pressures for the $x = 0.7$ compound. Instead, only small pressure dependence is observed, even though the $x = 0.7$ seems slightly more stable at higher pressures. This would suggest that the exchange mechanism that stabilises the magnetic order does not depend only on d_{Co-Co}. Of course, we should acknowledge the fact that the pressure applied in this study is hydrostatic and not uni-axial, even though chemical pressure can be considered equivalent to hydrostatic pressure. However, it is of course possible that a LRO is in fact stabilised at even higher pressures. Such premise may be confirmed by a pressure study on the $x = 0.75$ compound, which is closer to the LRO phase and should yield lower critical pressures. It is noted that while the frequency of the short range ordered phase is small, the highly damped nature does not stem from magnetic inhomogeniousity. Instead, the highly damped nature stems from a broad field distribution due to SRO formation, whereas the value of the frequency itself suggests that the internal field at the muon site is small.

The $x = 1$ compound on the other hand exhibits a strong pressure dependence, where the external pressure destabilizes the magnetic order. Such destabilizing with pressure was also observed for $x = 0.9$ and 0.8 compounds, even though it is much weaker. A simple and rough extrapolation would suggest that the long range order is fully suppressed at around 50 and 100 kbar for $x = 0.9$ and 0.8, respectively. The much weaker pressure dependence of the $x = 0.9$ and 0.8 compounds supports the fact that the magnetic order may be established by exchanges other than simply the inter-plane Co ion interaction.

The pressure clearly induces a transition in the $x = 1$ compound, from magnetically long-range order to a magnetically disordered state. Suppression of magnetic order under applied external pressure is a signature of quantum criticality[19,20]. Of course, for such scenario one would expect that T_N would be more smoothly driven towards $T = 0$ K, which is not really seen here. That being said, the related compound $CrRh_2Si_2$[21] or the d-electron antiferromagnet $Cr_{1-x}V_x$[22] were both shown to exhibit a second order nature, despite a similar abrupt decrease. Figure 2b shows the order parameter evolution as a function of pressure for the $x = 1$ compound. Here, an abrupt decrease of the order parameter is observed between 9.2 and 9.7 kbar. In other words, the suppression of the magnetic order under pressure is not likely to be quantum critical. This is also coherent with the fact that Fermi liquid behaviour is observed through out the pressure range, based on resistivity measurements[12]. Instead, the transition is first order in nature and thus most likely driven by a structural component. In fact, similar compounds have been shown to undergo first order transition under pressure, e.g. $EuCo_2P_2$ and $SrNi_2P_2$ but at higher temperatures[23].

Since a missing fraction is only present just below p_{c2} and not above, we may conclude that the origin behind the missing fraction is magnetic. In other words, the missing fraction is stemming from changes in the magnetic environment. Such behaviour would be consistent with the sample undergoing AF-FM transition under pressure above 6 kbar ($p_{c1} \approx 8$ kbar). Typically, missing fractions are also more commonly observed for FM structures rather than in AF. Although, this is not a general rule. One could perhaps expect FM correlations to emerge under pressure at lower temperatures given that FM correlations seem to be present at ambient pressure above T_N[24]. In fact, magnetisation measurements as a function of magnetic fields[10] suggested small values of spontaneous magnetization to be present for $0.8 < x < 0.95$ ($\sim 0.05\mu_B$/Co for $x = 0.85$). The ground state was asserted to be a slightly complicated AF order with a small FM component. A similar FM component was not observed for $x = 1$. Since the ground states of these compounds are dependent on the interlayer coupling, it may be that hydrostatic pressure induces similar FM interaction on the $x = 1$ compound, which result in FM island formation under pressure.

The related compound $LaCo_2P_2$ is an itinerant FM at ambient pressure[25,26]. While any pressure dependent measurement is missing for $LaCo_2P_2$, a second phase emerged in the itinerant FM UGe_2 at lower temperature close to p_C[27], similar to what is observed for the $x = 1$ compound. Quantum critical points for antiferromagnets are widely studied and are in general well understood. The situation for FM compounds is however not as straight forward. Even though there are no direct limitation for a FM to exhibit a QCP[28], many real materials show instead first order transitions at low temperatures[29,30]. In fact, theoretical studies have suggested that itinerant FM compounds at $T = 0$ K undergo first order transitions[31,32] in order to minimize the free energy. Given that FM islands are formed in the $x = 1$ compound close to p_{c2}, the transition may be driven by correlation effects that minimises the free energy[31]. Since a tricritical point is expected close to the first order transition, it will be interesting to perform a magnetic field dependence on the $x = 1$ compound close to p_C at low temperatures.

Resistivity measurements on the x=1 compound under pressure revealed a change in its derivative at 8.9 kbar below 50 K[12], which was slowly suppressed with pressure. While the details and the origin remained unsolved, such feature is here clearly revealed to be of magnetic origin. This is based on the fact that an additional exponential component manifests the ZF time spectrum (Fig. 3) and that A_{TF} (Fig. 6) reveals an anomaly around this pressure ($p_{c1} \approx 8$ kbar) and temperature (which in turn is a consequence of such exponential). Since the amount of missing fraction is temperature independent at $p = 9.7$ kbar (Fig. 3), the initial faster relaxation at $p = 9.7$ kbar should yield some clues regarding the second phase that manifests itself at low temperatures (below $T_i \approx 20$ K) and above $p_{c1} \approx 8$ kbar.

In order to comprehend the second phase present at high pressure and low temperature, it is imperative to unveil the microscopic origin of the exponential. Unfortunately, the presence of the missing fraction makes the determination challenging. Regardless, lets first point out that there exist mixed fractions at this pressure: a missing fraction, a disordered phase (A_{PM}) and a fraction of muons depolarising in a fast exponential manner, that also changes with temperature. With this in mind, we shall propose few scenarios to the origin of the exponential. (1) The missing fraction is resulting from (ferro)magnetic islands (FMI). In this case, part of the muons will be situated in the disordered phase that is relatively close to two separate yet correlated magnetic islands. The inter-island correlation should depolarise the moun ensemble in an exponential manner that is different from the disordered phase. This scenario implies that some islands merge at lower temperatures (below $T_i \approx 20$ K), or the inter-island correlations are suppressed at lower temperatures for reasons unknown. (2) The exponential is a reminiscence of the missing fraction. It might be that oscillations/fluctuations hidden as a missing fraction is "spilled over" to the time window of μ^+SR. This would imply that the correlation times changes as the temperature is lowered. In other words, the missing fraction is somewhat fluctuating at higher temperatures, that becomes more static at lower temperature. (3) The muon site coordinates might have temperature dependencies at this pressure. Similar to how the muon sites can be pressure dependent, the temperature dependence of it could result in re-population among different sites. This implies that the low temperature phase and high pressure phase is driven by a structural component or a spin structure reorientation.

Given the structural and magnetic degree of freedom present in the $x = 1$ compound, it may be that several processes discussed above are viable. In order to discern one scenario from another, it is of high interest to perform high pressure XRD, high pressure magnetisation and neutron diffraction. Although, since the magnetic phases seem to form island like structures, detailed experimental study might prove difficult. We wish to stress that the complex temperature dependence of $A_{TF}(T)$ was not observed for the $x \neq 1$ compounds. In other words, impure samples or chemical disorder are not likely the underlying reason behind the features observed here. Especially since the pure $x = 1$ compounds are in general cleaner than chemically doped samples. Here, we should emphasize that μ^+SR is able to detect magnetic volume fractions in a sample. To conclude, we propose that the intermediate phase emerging above $p_{c1} \approx 8$ kbar consists of ferromagnetic islands (FMI) existing within a disordered phase. Further, such FMI undergo an additional transition between a high- (FMI-①) and low-temperature (FMI-②) state at $T_i \approx 20$ K. It should also be emphasized that the values of $p_{c1} \approx 8$ kbar and $T_i \approx 20$ K are approximated from a combination of ZF/TF μ^+SR data (with limited number of pressure points) in combination with the resistivity data from Ref.[12]. The presented numbers should therefore be taken as estimates and further detailed studies are necessary to more accurately determine the phase boundaries. However, $p_{c2} \approx 9.8$ kbar could be considered slightly more well defined.

Finally, we wish to discuss nature of the high pressure phase (above $p_{c2} \approx 9.8$ kbar). The resistivity above such critical pressure revealed a hump in the data[12]. Such 'hump temperature' was increasing with higher pressures. One suggestion was that it may be related to a broad magnetic transition, like seen in the related compounds $CaNi_{1-x}Co_xP_2$[33], $BaFe_{1-x}Cr_xAs_2$[34] and $BaFe_{1-x}Mn_xAs_2$[35]. However, such conclusion can be readily excluded based on this μ^+SR study. Instead, it might be that strong electron coupling is behind the such resistivity hump, like in Nb_3Sn and Nb_3Sb[36], which was also one of the suggestion of Ref.[12].

Conclusions

The pressure and temperate dependence on the magnetic nature of $Sr_{1-x}Ca_xCo_2P_2$ for $x = 1$, 0.9, 0.8 and 0.7 has been investigated by muon spin rotation, relaxation and resonance (μ^+SR). The weak pressure dependencies for the compounds $x \neq 1$ suggests that the rich phase diagram of $Sr_{1-x}Ca_xCo_2P_2$ at ambient pressure may not only be due to chemical pressure effects. The $x = 1$ compound on the other hand exhibits strong pressure effects, where the long range magnetic order present at ambient pressure become fully suppressed at $p_{c2} \approx 9.8$ kbar. Intriguingly, two additional phases emerge already just below the critical region, occupying the phase space above $p_{c1} \approx 8$ kbar and below $p_{c2} \approx 9.8$ kbar. Since μ^+SR is sensitive to magnetic volume fractions, such phase was proposed to be (ferro)magnetic islands (FMI) co-existing within a disordered phase. It is also revealed that such phase consists of a high- (FMI-①) and a low-temperature (FMI-②) region, respectively, with a phase boundary at $T_i \approx 20$ K.

Methods

$Sr_{1-x}Ca_xCo_2P_2$ polycrystalline samples were synthesised in a two step reaction from the base elements; P, Sr, Ca, and Co. At first, Sr, Ca, Co were individually put together with P in an evacuated quartz tube to facilitate a solid state reaction at 800 °C and 700 °C to produce SrP, CaP and Co_2P. $Sr_{1-x}Ca_xCo_2P_2$ was then synthesized via a solid-state reaction between SrP, CaP, and Co_2P at 1000°C for 20 hours in Ar atmosphere. Detailed information about the synthesis protocol is found in Ref.[24].

The μ^+SR measurements were performed at the GPD instrument on the μE1 beamline at the SμS muon source of Paul Scherrer Institute (PSI), Switzerland. Hydrostatic pressures up to 23 kbar were achieved by using a piston cylinder cell made of MP35 alloys. Temperatures down to $T = 2$ K were achieved using a ^{4}He flow cryostat. Some of the measurements were conducted using a He-3 insert to reach temperatures $T = 0.3$ K. Three pressed pellets of the powder samples were stacked (5.9 mm diameter and 13 mm total height) for each measurement and inserted into the pressure cell. Daphne oil was used as the pressure medium in order to achieve the hydrostatic pressure. The pressure of the sample at low temperatures was accurately determined via AC susceptibility measurements of the superconducting transition temperature for a small indium wire located at the bottom of (inside) the pressure cell[13,19,37]. Finally, the free analysis software `musrfit`[38] was used to analyzed the μ^+SR data.

Data availibility

All data needed to evaluate the conclusions in the paper are present in the paper. Additional data requests should be addressed to the corresponding authors.

Received: 22 July 2022; Accepted: 30 September 2022
Published online: 20 October 2022

References

1. Johrendt, D. *et al.* LMTO band structure calculations of ThCr2Si2-type transition metal compounds. *J. Solid State Chem.* **130**, 254. https://doi.org/10.1006/jssc.1997.7300 (1997).
2. Reehuis, M., Jeitschko, W., Kotzyba, G., Zimmer, B. & Hu, X. Antiferromagnetic order in the ThCr2Si2 type phosphides CaCo2P2 and CeCo2P2. *J. Alloys Compd.* **266**, 54. https://doi.org/10.1016/S0925-8388(97)00486-6 (1998).
3. Hoffmann, R. & Zheng, C. Making and breaking bonds in the solid state: The ThCr2Si2 structure. *J. Phys. Chem.* **89**, 4175 (2002).
4. Rotter, M. *et al.* Spin-density-wave anomaly at 140 K in the ternary iron arsenide BaFe $_2$ As $_2$. *Phys. Rev. B* **78**, 020503. https://doi.org/10.1103/PhysRevB.78.020503 (2008).
5. Tan, X. *et al.* Complex magnetic phase diagram with multistep spin-flop transitions in $La_{0.25}Pr_{0.75}Co_2P_2$. *Phys. Rev. B* **95**, 024428. https://doi.org/10.1103/PhysRevB.95.024428 (2017).
6. Rotter, M., Tegel, M. & Johrendt, D. Superconductivity at 38 K in the Iron Arsenide $(Ba_{1-x}K_x)Fe_2As_2$. *Phys. Rev. Lett.* **101**, 107006. https://doi.org/10.1103/PhysRevLett.101.107006 (2008).
7. Torikachvili, M. S., Bud'ko, S. L., Ni, N. & Canfield, P. C. Pressure induced superconductivity in $CaFe_2As_2$. *Phys. Rev. Lett.* **101**, 057006. https://doi.org/10.1103/PhysRevLett.101.057006 (2008).
8. Reehuis, M. & Jeitschko, W. Structure and magnetic properties of the phosphides CaCo2P2 and LnT2P2 with ThCr2Si2 structure and LnTP with PbFCl structure (Ln = Lanthanoids, T = Fe Co, Ni). *J. Phys. Chem. Solids* **51**, 961. https://doi.org/10.1016/0022-3697(90)90039-I (1990).
9. Kreyssig, A. *et al.* Pressure-induced volume-collapsed tetragonal phase of CaFe $_2$ As $_2$ as seen via neutron scattering. *Phys. Rev. B* **78**, 184517. https://doi.org/10.1103/PhysRevB.78.184517 (2008).
10. Jia, S., Williams, A. J., Stephens, P. W. & Cava, R. J. Lattice collapse and the magnetic phase diagram of Sr $_{1-x}$ Ca $_x$ Co $_2$ P $_2$. *Phys. Rev. B* **80**, 165107. https://doi.org/10.1103/PhysRevB.80.165107 (2009).
11. Sugiyama, J. *et al.* Variation of magnetic ground state of determined with μ^+SR. *Phys. Rev. B* **91**, 69. https://doi.org/10.1103/PhysRevB.91.144423 (2015).
12. Baumbach, R. E. *et al.* Suppression of antiferromagnetism by pressure in CaCo $_2$ P $_2$. *Phys. Rev. B* **89**, 094408. https://doi.org/10.1103/PhysRevB.89.094408 (2014).
13. Khasanov, R. *et al.* High pressure research using muons at the Paul Scherrer Institute. *High Press. Res.* **36**, 140. https://doi.org/10.1080/08957959.2016.1173690 (2016).
14. Boekema, C. *et al.* Muon bonding versus muonium formation: Muon-spin-relaxation in α-Al2O3. *Hyperfine Interact.* **32**, 667. https://doi.org/10.1007/BF02394971 (1986).
15. Cox, S. F. J. *et al.* Oxide muonics: I. Modelling the electrical activity of hydrogen in semiconducting oxides. *J. Phys. Condens. Matter* **18**, 1061. https://doi.org/10.1088/0953-8984/18/3/021 (2006).
16. Forslund, O. K. Your muonium is μ-drogen. in *Proceedings of the 14th International Conference on Muon Spin Rotation, Relaxation and Resonance* (μSR2017). https://doi.org/10.7566/JPSCP.21.011066 (2017).
17. Forslund, O. K. *et al.* Revisiting the *A*-type antiferromagnet $NaNiO_2$ with muon spin rotation measurements and density functional theory calculations. *Phys. Rev. B* **102**, 184412. https://doi.org/10.1103/PhysRevB.102.184412 (2020).
18. Forslund, O. K. *et al.* Co-existence of short- and long-range magnetic order in LaCo2P2. *Phys. Scr.* **96**, 125864. https://doi.org/10.1088/1402-4896/ac3cf9 (2021).
19. Forslund, O. K. *et al.* Magnetic phase diagram of K2Cr8O16 clarified by high-pressure muon spin spectroscopy. *Sci. Rep.* **9**, 1141. https://doi.org/10.1038/s41598-018-37844-5 (2019).
20. Sugiyama, J. *et al.* Magnetic phase boundary of $BaVS_3$ clarified with high-pressure μ^+SR. *Phys. Rev. B* **101**, 174403. https://doi.org/10.1103/PhysRevB.101.174403 (2020).
21. Movshovich, R., Graf, T., Mandrus, D., Hundley, M., Thompson, J., Fisher, R., Phillips, N., & Smith, J. Response of CeRh2Si2 to pressure, Phys. B Condens. Matter **223-224**, 126. https://doi.org/10.1016/0921-4526(96)00058-0 (1996) (proceedings of the international conference on strongly correlated electron systems).
22. Lee, M., Husmann, A., Rosenbaum, T. F. & Aeppli, G. High resolution study of magnetic ordering at absolute zero. *Phys. Rev. Lett.* **92**, 187201. https://doi.org/10.1103/PhysRevLett.92.187201 (2004).
23. Huhnt, C., Schlabitz, W., Wurth, A., Mewis, A. & Reehuis, M. First-order phase transitions in $EuCo_2P_2$ and $SrNi_2P_2$. *Phys. Rev. B* **56**, 13796. https://doi.org/10.1103/PhysRevB.56.13796 (1997).
24. Imai, M. *et al.* Anomalous itinerant-electron metamagnetic transition in the layered $Sr_{1-x}Ca_xCo_2P_2$ system. *Phys. Rev. B* **90**, 014407. https://doi.org/10.1103/PhysRevB.90.014407 (2014).
25. Mörsen, E., Mosel, B., Müller-Warmuth, W., Reehuis, M. & Jeitschko, W. Mössbauer and magnetic susceptibility investigations of strontium, lanthanum and europium transition metal phosphides with ThCr2Si2 type structure. *J. Phys. Chem. Solids* **49**, 785. https://doi.org/10.1016/0022-3697(88)90030-3 (1988).
26. Reehuis, M., Ritter, C., Ballou, R. & Jeitschko, W. Ferromagnetism in the ThCr2Si2 type phosphide LaCo2P2. *J. Magnet. Magnet. Mater.* **138**, 85. https://doi.org/10.1016/0304-8853(94)90402-2 (1994).
27. Pfleiderer, C. & Huxley, A. D. Pressure dependence of the magnetization in the ferromagnetic superconductor UGe_2. *Phys. Rev. Lett.* **89**, 147005. https://doi.org/10.1103/PhysRevLett.89.147005 (2002).
28. Steppke, A. *et al.* Ferromagnetic quantum critical point in the heavy-fermion metal $YbNi_4(P_{1-x}As_x)_2$. *Science* **339**, 933. https://doi.org/10.1126/science.1230583 (2013).
29. Pfleiderer, C., McMullan, G. J., Julian, S. R. & Lonzarich, G. G. Magnetic quantum phase transition in MnSi under hydrostatic pressure. *Phys. Rev. B* **55**, 8330. https://doi.org/10.1103/PhysRevB.55.8330 (1997).
30. Uhlarz, M., Pfleiderer, C. & Hayden, S. M. Quantum phase transitions in the itinerant ferromagnet $ZrZn_2$. *Phys. Rev. Lett.* **93**, 256404. https://doi.org/10.1103/PhysRevLett.93.256404 (2004).
31. Belitz, D., Kirkpatrick, T. R. & Vojta, T. First order transitions and multicritical points in weak itinerant ferromagnets. *Phys. Rev. Lett.* **82**, 4707. https://doi.org/10.1103/PhysRevLett.82.4707 (1999).
32. Chubukov, A. V., Pépin, C. & Rech, J. Instability of the quantum-critical point of itinerant ferromagnets. *Phys. Rev. Lett.* **92**, 147003. https://doi.org/10.1103/PhysRevLett.92.147003 (2004).
33. Jia, S., Chi, S., Lynn, J. W. & Cava, R. J. Magnetic and structural properties of Ca (Fe $_{1-x}$ Co $_x$)$_2$ P $_2$ and Ca (Ni $_{1-x}$ Co $_x$)$_2$ P $_2$. *Phys. Rev. B* **81**, 214446. https://doi.org/10.1103/PhysRevB.81.214446 (2010).
34. Marty, K. *et al.* Competing magnetic ground states in nonsuperconducting $Ba(Fe_{1-x}Cr_x)_2As_2$ as seen via neutron diffraction. *Phys. Rev. B* **83**, 060509. https://doi.org/10.1103/PhysRevB.83.060509 (2011).

35. Thaler, A. *et al.* Physical and magnetic properties of $Ba(Fe_{1-x}Mn_x)_2As_2$ single crystals. *Phys. Rev. B* **84**, 144528. https://doi.org/10.1103/PhysRevB.84.144528 (2011).
36. Fisk, Z. & Webb, G. W. Saturation of the high-temperature normal-state electrical resistivity of superconductors. *Phys. Rev. Lett.* **36**, 1084. https://doi.org/10.1103/PhysRevLett.36.1084 (1976).
37. Andreica, D. *Magnetic Phase Diagram in some Kondo-Lattice Compounds: Microscopic and Macroscopic Studies*. Ph.D. Thesis, IPP/ETH-Zurich (2001).
38. Suter, A. & Wojek, B. M. Musrfit: A free platform-independent framework for μSR data analysis. *Phys. Proc.* **30**, 69. https://doi.org/10.1016/j.phpro.2012.04.042 (2012).

Acknowledgements

This research was supported by the Swedish Research Council (VR) via a Neutron Project Grant (Dnr. 2021-06157) and the Carl Tryggers Foundation for Scientific Research (CTS-18:272). D.A. acknowledges financial support from the Romanian UEFISCDI project PN-III-P4-ID-PCCF-2016-0112, Contract Nr. 6/2018. Y.S. is funded by VR through a Starting Grant (Dnr. 2017-05078) as well as the Chalmers Area of Advance-Materials Science. J.S. acknowledges support from Japan Society for the Promotion Science (JSPS) KAKENHI Grants No. JP18H01863 and No. JP20K21149.

Author contributions

The experiment was conceived by M.M. and conducted by O.K.F., D.A., Y.S., Z.G., Z.S., R.K., J.S. and M.M. The samples were grown by M.I., C.M. and K.Y. O.K.F. analysed the data and wrote the manuscript. All authors contributed to the final draft.

Funding

Open access funding provided by Royal Institute of Technology.

Competing interests

The authors declare no competing interests.

Additional information

Correspondence and requests for materials should be addressed to O.K.F.

Reprints and permissions information is available at www.nature.com/reprints.

Publisher's note Springer Nature remains neutral with regard to jurisdictional claims in published maps and institutional affiliations.